

# DEFormer: DCT-driven Enhancement Transformer for Low-light Image and Dark Vision

1<sup>nd</sup> Xiangchen Yin\*

*University of Science and Technology of China  
Institute of Artificial Intelligence,  
Hefei Comprehensive National Science Center  
Hefei 230601, China  
E-mail: yinxianchen@mail.ustc.edu.cn*

2<sup>nd</sup> Zhenda Yu\*

*Anhui University  
Institute of Artificial Intelligence,  
Hefei Comprehensive National Science Center  
Hefei 230601, China  
E-mail: wa22201140@stu.ahu.edu.cn*

3<sup>rd</sup> Xin Gao

*School of Vehicle and Mobility,  
Tsinghua University  
Beijing 230601, China  
E-mail: bqt2000405024@student.cumtb.edu.cn*

4<sup>th</sup> Xiao Sun<sup>#</sup>

*Institute of Artificial Intelligence,  
Hefei Comprehensive National Science Center  
School of Computer Science and Information Engineering,  
Hefei University of Technology  
Hefei 230601, China  
E-mail: sunx@hfut.edu.cn*

**Abstract**—Low-light image enhancement restores colors and details of single image and improves high-level visual tasks. However, restoring the lost details in the dark area is a challenge by only relying on the RGB domain. In this paper, we introduce frequency as a new clue into the network and propose a DCT-driven enhancement transformer (DEFormer) framework. First, we propose a learnable frequency branch (LFB) for frequency enhancement contains DCT processing and curvature-based frequency enhancement (CFE) to represent frequency features. In addition, we propose a cross domain fusion (CDF) for reducing the differences between the RGB domain and the frequency domain. Our DEFormer has achieved advanced results in both the LOL and MIT-Adobe FiveK datasets and improved the performance of dark detection.

**Index Terms**—Low-light Image Enhancement; Discrete Cosine Transform; Frequency Learning; Transformer

## I. INTRODUCTION

Low-light images have many dark areas, which result in noise, lose details and bring a negative visual experience. Low-light images make the performance of high-level visual tasks decline (such as object detection [1]–[3], face detection [4]–[6]). Many low-light image enhancement (LLIE) methods have been proposed recently. Based on the Retinex theory [7], some methods [8]–[10] decompose the image into reflection components and illumination components and enhance them. However, traditional methods with manual feature learning has large limitations and poor generalization. Currently, there are also some CNN based [11]–[13] and transformer based [14]–[16] works proposed for bad scenes such as night, which improve downstream tasks in dark condition.

Discrete cosine transform (DCT) is an important part of frequency signal analysis, which has been proven effective in computer vision [17]–[19]. Inspired by the frequency [20]–[22], in this paper we propose a DCT-driven enhancement transformer (DEFormer) for low-light enhancement. We propose a learnable frequency branch (LFB) that contains DCT processing and curvature-based frequency enhancement (CFE) to embed information of DCT. In addition, we propose a cross domain fusion (CDF) for reducing the differences between different domains. We adopt LOL [23] and MIT-Adobe FiveK [24] datasets for low-light enhancement experiments and the results show that DEFormer achieves advanced performance comparing with other state-of-the-art methods. We achieve effective improvements on the ExDark [3] datasets through end-to-end finetuning. The performance comparison of different SOTA methods is shown in Fig. 1 (c).

Our contributions are summarized as follows:

- Jointing DCT with transformer, we propose a DCT-driven enhancement transformer (DEFormer) for low-light enhancement and we design a learnable frequency branch (LFB) to embed frequency clue.
- We propose curvature-based frequency enhancement (CFE) to adaptively focus on frequency-band channels with rich textures. In addition, we propose a cross domain fusion (CDF) to fuse the features of RGB domain and frequency domain.
- DEFormer has obtained advanced results on public datasets, and end-to-end training of DEFormer and detectors has a outstanding performance improvement for downstream dark detection tasks.

\* denotes equal contributions.

# denotes the corresponding author.

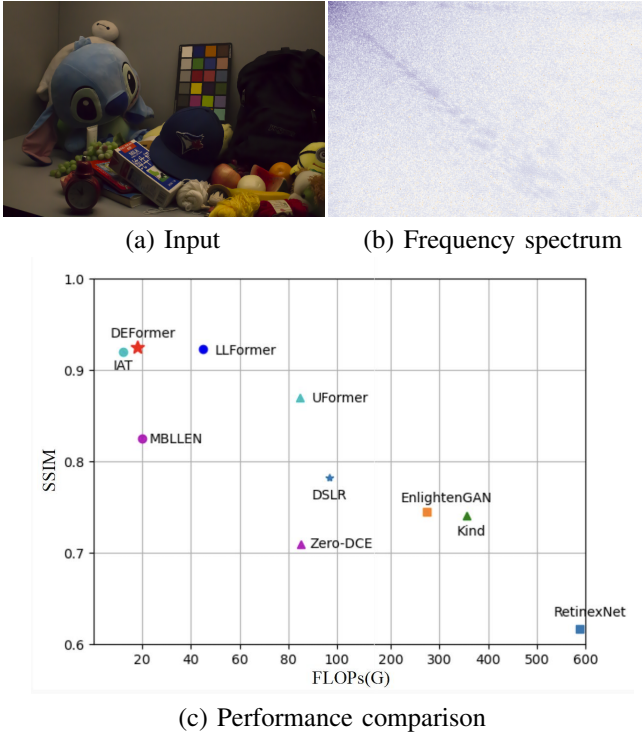


Fig. 1. (a) represents the input, (b) represents the frequency spectrum after DCT processing. The DCT coefficient matrix concentrate the energy of the image signal, so as to realize the effective analysis of the image signal. (c) represents the performance comparison between the SOTA methods in the MIT-Adobe FiveK dataset, the x-axis represents Flops and the y-axis represents SSIM.

## II. METHOD

The overview of DEFormer is shown in Fig. 2. Taking a low-light image  $I \in R^{H \times W \times 3}$  as input, first we extract the shallow features  $F_0 \in R^{H \times W \times 16}$  through a  $3 \times 3$  convolution block. Then we apply two transformer blocks to predict a multiple map and an add map respectively and get the feature of the RGB domain  $F_{rgb} \in R^{H \times W \times 16}$ . In the learnable frequency branch (LFB), we first perform DCT processing on  $I$ , then divide it into high and low parts with the curvature-based frequency enhancement (CFE) and enhance them respectively, throughout tensor concat we obtain the features  $F_1 \in R^{H/8 \times W/8 \times 192}$ . We reshape  $F_1$  to  $R^{H \times W \times 3}$  and extract features of the frequency domain  $F_f \in R^{H \times W \times 16}$ . We reduce the differences of domain between  $F_{rgb}$  and  $F_f$  by cross fusion in cross domain fusion (CDF). After fusion we apply a transformer block to extract deep features  $F_2 \in R^{H \times W \times 16}$ . Finally, we use a  $3 \times 3$  convolution and Leaky ReLU function to obtain the enhanced image  $\hat{I} \in R^{H \times W \times 3}$ .

### A. Learnable Frequency Branch

Recovering lost details in dark regions is difficult with only in the RGB domain. Therefore, we apply DCT to introduce the frequency as a additional clue. The learnable frequency branch (LFB) consists of DCT processing and curvature-based frequency enhancement (CFE), as shown in Fig. 2.

**DCT process.** Given an RGB image  $x \in R^{H \times W \times 3}$ , convert it to the color space of YCbCr to get  $x_{ycbcr} \in R^{H \times W \times 3}$ . Then we split  $x_{ycbcr}$  in each channel according to the patch of  $8 \times 8$  to get  $p_{i,j} \in R^{8 \times 8}$ ,  $1 \leq i \leq H/8, 1 \leq j \leq W/8$ . After that we process each patch through slide window DCT to obtain local frequency information. DCT has the characteristics of energy concentration, as shown in Fig. 1 (b), the information is concentrated in the upper left corner of the spectrum, which is also helpful for the separation of noise. The DCT processing of the image is described as

$$F(u, v) = \frac{2}{\sqrt{HW}} \sum_{i=0}^{H-1} \sum_{j=0}^{W-1} f(i, j) \cos \frac{u(2i+1)\pi}{2H} \cos \frac{v(2j+1)\pi}{2W} \quad (1)$$

where  $1 \leq u \leq H$  and  $1 \leq v \leq W$ ,  $F(*)$  is the frequency signals and  $f(*)$  is the RGB signals. We attribute all the components of the same frequency band to a channel and get the feature  $x_f \in R^{H/8 \times W/8 \times 192}$  in the frequency domain.

**Curvature-based frequency enhancement.** In 2D surfaces, the average curvature can represent the surface roughness, which originates from the details of the image. We measure different frequency bands on the channel based on the curvature to obtain the quantization parameter of the feature on each channel. We adopt a linear method to reduce the amount of curvature calculation, this process is described as

$$C \approx \omega \cdot X \quad (2)$$

where  $X \in R^{H \times W \times C}$  represents the frequency feature,  $C \in R^{H \times W \times C}$  represents the curvature map,  $\omega$  represents initial weight, adapting to the network through microscopic during the training process.

$$\omega = \begin{bmatrix} -\frac{1}{16} & \frac{5}{16} & -\frac{1}{16} \\ \frac{5}{16} & -1 & \frac{5}{16} \\ -\frac{1}{16} & \frac{5}{16} & -\frac{1}{16} \end{bmatrix} \quad (3)$$

then we sum the curvature map in two dimensions to obtain an energy vector  $E \in R^{1 \times 1 \times C}$  representing each channel. We sort  $E$  and divide the frequency features into high part and low part according to 3:1. In high part we apply several  $\{Conv, BN, ReLU\}$  and skip connection to enhance frequency domain information. In the low part, we use a  $3 \times 3$  convolution for simple calibration and the two parts are concat in channel dimensions. Finally, we reshape the enhanced  $X$  to  $R^{H \times W \times 3}$  and use a convolution to get the enhanced frequency domain feature  $F_f \in R^{H \times W \times 16}$ .

### B. Cross Domain Fusion

We design a cross domain fusion (CDF) to reduce the differences between the frequency domain  $F_f$  and the feature of the RGB domain  $F_{rgb}$ , as shown in Fig. 3. First, we obtain global information by global average pooling along the channels and obtain attention vectors through two filters respectively. This process is described as

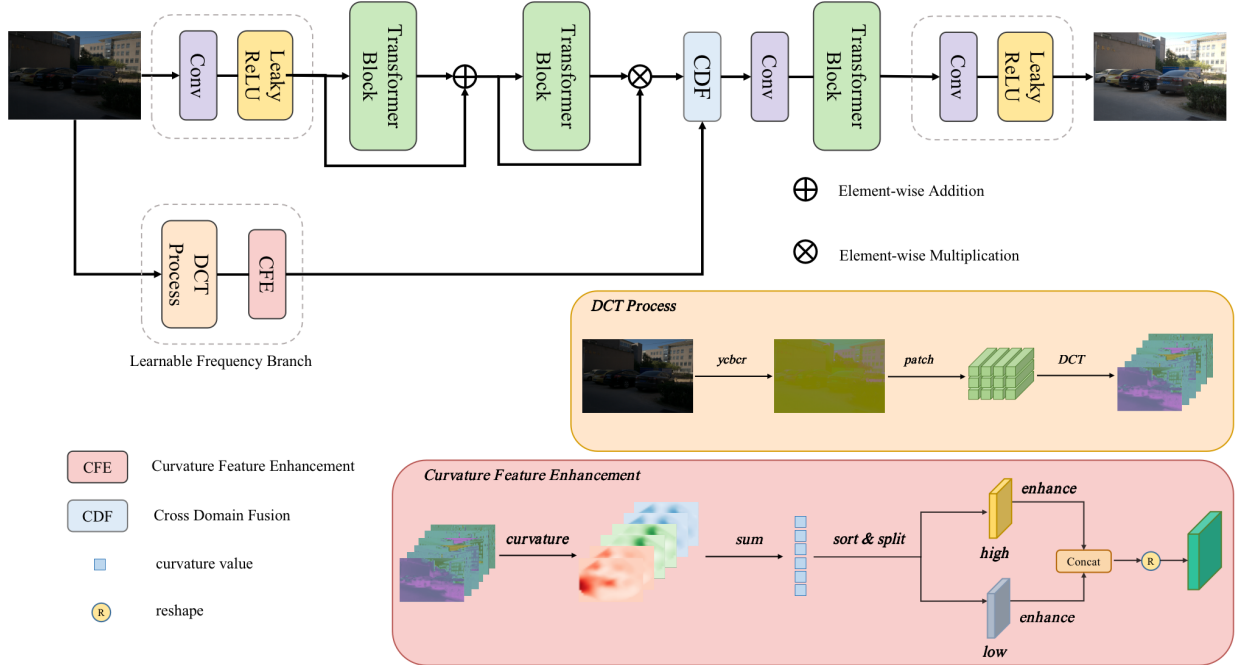


Fig. 2. Overview of DEFormer. Two transformer blocks are used to extract shallow features. In the learnable frequency branch (LFB), we introduce frequency clues through DCT processing and curve-based frequency enhancement. In cross domain fusion, the difference between RGB domain and frequency domain is reduced through cross fusion.

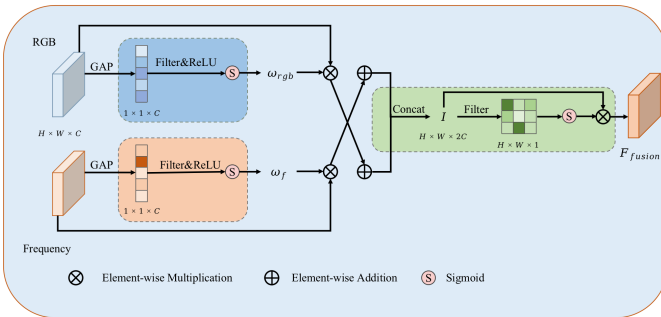


Fig. 3. Details of cross domain fusion (CDF). We first complement the information between different domains through cross-fusion, and control the spatial information through a soft attention to reduce noise propagation.

$$\omega_{rgb} = \sigma(Filter(GAP(F_{rgb}))) \quad (4)$$

$$\omega_f = \sigma(Filter(GAP(F_f))) \quad (5)$$

where  $\sigma$  represents the sigmoid function, and we need to scale the weights to  $[0, 1]$ . GAP represents global average pooling. The weights can effectively suppress the importance of the noisy part. The cross fusion is described as

$$I = relu(\omega_{rgb} \cdot F_{rgb} + F_f || \omega_f \cdot F_f + F_{rgb}) \quad (6)$$

where  $I$  represents the features of the initial fusion and  $||$  represents the tensor concat. This process effectively reduces large differences between domains. We apply a  $1 \times 1$  convolution



Fig. 4. Visualization of dark object detection on ExDark dataset. MBLLEN directly predict the enhanced image and apply detector training, and DEFormer uses end-to-end training.

layer and sigmoid function to obtain the information of  $I$  in the spatial dimension to get a more robust fusion representation. The process is as follows

$$F_{fusion} = \sigma(Filter(I)) \cdot I \quad (7)$$

where  $F_{fusion}$  is fused feature.

### III. EXPERIMENTS

For low-light enhancement, we apply the LOL and MIT-Adobe FiveK datasets. We conduct our experiments under Ubuntu 18.04, Pytorch, RTX 3090. We use SGD and set the initial learning rate and weight decay to 0.0001 and 0.00005, respectively. During training, epoch is set to 1000, and batch-size is set to 8. We use PSNR, SSIM, parameters and Flops for evaluation.

#### A. Comparison of Low-light Enhancement

We quantitatively compared DEFormer with other state-of-art methods such as RetinexNet [23], Uformer [29], LLFormer

TABLE I

COMPARISON OF LOW-LIGHT ENHANCEMENT MODEL ON LOL AND MIT-ADobe FiveK DATASETS. THE FIRST BEST RESULT AND THE SECOND BEST RESULT IS MARKED AS BLUE AND GREEN RESPECTIVELY.

Model	LOL		MIT-Adobe FiveK		Parameters(M)	FLOPs(G)
	PSNR	SSIM	PSNR	SSIM		
RetinexNet [23]	16.77	0.562	12.51	0.671	0.84	587.47
Kind [25]	20.86	0.790	14.54	0.741	8.16	356.72
Zero-DCE [26]	14.86	0.589	13.20	0.709	0.08	84.99
EnlightenGAN [27]	17.48	0.677	13.26	0.745	8.64	273.24
IAT [28]	21.87	0.788	25.10	0.920	0.09	12.16
UFormer [29]	19.39	0.786	21.92	0.870	5.29	84.94
Restormer [30]	22.37	0.816	24.92	0.911	26.13	281.98
LLFormer [31]	23.64	0.816	25.75	0.923	24.55	45.04
PairLIE [32]	19.51	0.736	-	-	3.42	179.58
DEFormer (Ours)	23.73	0.821	25.14	0.925	2.25	17.96

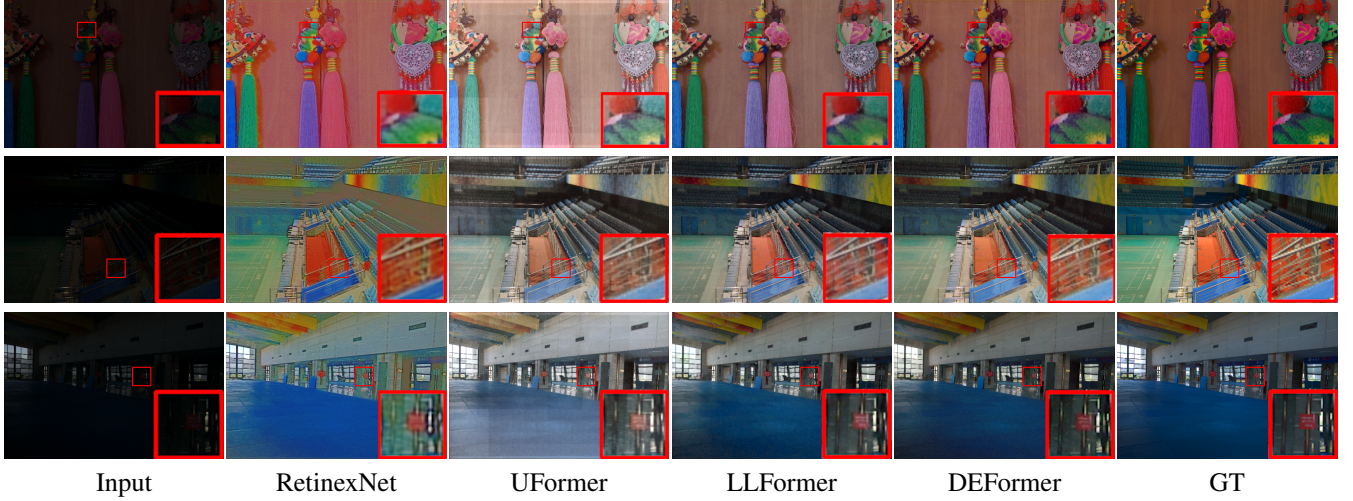


Fig. 5. Visualization of different low-light image enhancement methods on LOL dataset. Each row is a different image comparison. We advise that zoom in to observe the details.

TABLE II

ABLATION STUDY FOR DEFORMER. "FI" REPRESENTS FREQUENCY INFORMATION, "CFE" REPRESENTS CURVATURE-BASED FREQUENCY ENHANCEMENT, "CDF" REPRESENTS CROSS DOMAIN FUSION.

Component	PSNR/SSIM	FLOPs (G)	Para(M)
Baseline	21.12/0.793	13.54	1.24
LFB(FI)	21.57/0.797	13.78	1.28
LFB(CFE+FI)	22.14/0.805	15.48	2.20
LFB+CDF	23.73/0.821	17.96	2.25

[31], and IAT [28]. The results are shown in Table I. Our DEFormer has achieved advanced results in both the LOL and MIT-Adobe FiveK datasets, with only 17.96G of parameters. We visualize the results of some SOTA models and DEFormer in the LOL dataset, as shown in Fig. 5, in contrast our method has high quality in both texture and color.

In addition, we fine-tune DEFormer and YOLOv3 detectors through end-to-end training and we visualize in ExDark datasets, as shown in Fig. 4. Our DEFormer has achieved effective improvement in the ExDark dataset, which is 2.1% higher than baseline in mAP, this shows that our model improves downstream visual tasks.

### B. Ablation Study

We conducted ablation studies on the LOL dataset, and the results are shown in Table II. We directly added the frequency domain information to the network, PSNR and SSIM increased by 0.45 and 0.004 respectively. After adopting the curvature-based frequency enhancement, PSNR and SSIM are 1.02 and 0.012 higher than the baseline, respectively. After using cross domain fusion, PSNR and SSIM have increased by 2.61 and 0.028, respectively. Overall, this ablation study shows that using frequency information as additional clue in the network is an effective solution.

### IV. CONCLUSIONS

In this paper, we propose DEFormer using frequency as a new clue, which mainly includes learnable frequency branch (LFB) and cross domain fusion (CDF). Extensive experiments show that DEFormer outperforms state-of-the-art methods in low-light enhancement and improves downstream detection tasks well as preprocessing.

### REFERENCES

[1] T.-Y. Lin, M. Maire, S. Belongie, J. Hays, P. Perona, D. Ramanan, P. Dollár, and C. L. Zitnick, "Microsoft coco: Common objects in

context,” in *Computer Vision–ECCV 2014: 13th European Conference, Zurich, Switzerland, September 6–12, 2014, Proceedings, Part V 13*. Springer, 2014, pp. 740–755.

[2] X. Yin, Z. Yu, Z. Fei, W. Lv, and X. Gao, “Pe-yolo: Pyramid enhancement network for dark object detection,” 2023.

[3] Y. P. Loh and C. S. Chan, “Getting to know low-light images with the exclusively dark dataset,” *Computer Vision and Image Understanding*, vol. 178, pp. 30–42, 2019.

[4] W. Yang, Y. Yuan, W. Ren, J. Liu, W. J. Scheirer, Z. Wang, T. Zhang, Q. Zhong, D. Xie, S. Pu *et al.*, “Advancing image understanding in poor visibility environments: A collective benchmark study,” *IEEE Transactions on Image Processing*, vol. 29, pp. 5737–5752, 2020.

[5] W. Wang, X. Wang, W. Yang, and J. Liu, “Unsupervised face detection in the dark,” *IEEE Transactions on Pattern Analysis and Machine Intelligence*, vol. 45, no. 1, pp. 1250–1266, 2022.

[6] W. Wang, W. Yang, and J. Liu, “Hla-face: Joint high-low adaptation for low light face detection,” in *Proceedings of the IEEE/CVF Conference on Computer Vision and Pattern Recognition*, 2021, pp. 16 195–16 204.

[7] E. H. Land, “The retinex theory of color vision,” *Scientific american*, vol. 237, no. 6, pp. 108–129, 1977.

[8] M. Li, J. Liu, W. Yang, X. Sun, and Z. Guo, “Structure-revealing low-light image enhancement via robust retinex model,” *IEEE Transactions on Image Processing*, vol. 27, no. 6, pp. 2828–2841, 2018.

[9] S. Wang, J. Zheng, H.-M. Hu, and B. Li, “Naturalness preserved enhancement algorithm for non-uniform illumination images,” *IEEE transactions on image processing*, vol. 22, no. 9, pp. 3538–3548, 2013.

[10] T. Celik and T. Tjahjadi, “Contextual and variational contrast enhancement,” *IEEE Transactions on Image Processing*, vol. 20, no. 12, pp. 3431–3441, 2011.

[11] S. Kalwar, D. Patel, A. Aanegola, K. R. Konda, S. Garg, and K. M. Krishna, “Gdip: Gated differentiable image processing for object detection in adverse conditions,” in *2023 IEEE International Conference on Robotics and Automation (ICRA)*. IEEE, 2023, pp. 7083–7089.

[12] Y. Zheng, C. Zhong, P. Li, H.-a. Gao, Y. Zheng, B. Jin, L. Wang, H. Zhao, G. Zhou, Q. Zhang *et al.*, “Steps: Joint self-supervised nighttime image enhancement and depth estimation,” *arXiv preprint arXiv:2302.01334*, 2023.

[13] H. Wang, K. Xu, and R. W. Lau, “Local color distributions prior for image enhancement,” in *European Conference on Computer Vision*. Springer, 2022, pp. 343–359.

[14] S. Zhang, N. Meng, and E. Y. Lam, “Lrt: an efficient low-light restoration transformer for dark light field images,” *IEEE Transactions on Image Processing*, 2023.

[15] B. Zhang, J. Suo, and Q. Dai, “A complementary dual-backbone transformer extracting and fusing weak cues for object detection in extremely dark videos,” *Information Fusion*, vol. 97, p. 101822, 2023.

[16] H. Singh, S. Suman, B. N. Subudhi, V. Jakhetiya, and A. Ghosh, “Action recognition in dark videos using spatio-temporal features and bidirectional encoder representations from transformers,” *IEEE Transactions on Artificial Intelligence*, vol. 4, no. 6, pp. 1461–1471, 2022.

[17] H.-D. Lin and D.-C. Ho, “Detection of pinhole defects on chips and wafers using dct enhancement in computer vision systems,” *The International Journal of Advanced Manufacturing Technology*, vol. 34, pp. 567–583, 2007.

[18] K. Su, L. Cao, B. Zhao, N. Li, D. Wu, X. Han, and Y. Liu, “Dctvit: Discrete cosine transform meet vision transformers,” *Neural Networks*, vol. 172, p. 106139, 2024.

[19] X. Shen, J. Yang, C. Wei, B. Deng, J. Huang, X.-S. Hua, X. Cheng, and K. Liang, “Dct-mask: Discrete cosine transform mask representation for instance segmentation,” in *Proceedings of the IEEE/CVF conference on computer vision and pattern recognition*, 2021, pp. 8720–8729.

[20] J. Lee and H. Kim, “Discrete cosine transformed images are easy to recognize in vision transformers.” *IEIE Transactions on Smart Processing & Computing*, vol. 12, no. 1, pp. 48–54, 2023.

[21] Z. Wang, H. Luo, P. Wang, F. Ding, F. Wang, and H. Li, “Vtc-lfc: Vision transformer compression with low-frequency components,” *Advances in Neural Information Processing Systems*, vol. 35, pp. 13 974–13 988, 2022.

[22] B. N. Patro, V. P. Namboodiri, and V. S. Agnieszka, “Specformer: Frequency and attention is what you need in a vision transformer,” *arXiv preprint arXiv:2304.06446*, 2023.

[23] C. Wei, W. Wang, W. Yang, and J. Liu, “Deep retinex decomposition for low-light enhancement,” *arXiv preprint arXiv:1808.04560*, 2018.

[24] V. Bychkovsky, S. Paris, E. Chan, and F. Durand, “Learning photographic global tonal adjustment with a database of input/output image pairs,” in *CVPR 2011*. IEEE, 2011, pp. 97–104.

[25] Y. Zhang, J. Zhang, and X. Guo, “Kindling the darkness: A practical low-light image enhancer,” in *Proceedings of the 27th ACM international conference on multimedia*, 2019, pp. 1632–1640.

[26] C. Guo, C. Li, J. Guo, C. C. Loy, J. Hou, S. Kwong, and R. Cong, “Zero-reference deep curve estimation for low-light image enhancement,” in *Proceedings of the IEEE/CVF conference on computer vision and pattern recognition*, 2020, pp. 1780–1789.

[27] Y. Jiang, X. Gong, D. Liu, Y. Cheng, C. Fang, X. Shen, J. Yang, P. Zhou, and Z. Wang, “Enlightengan: Deep light enhancement without paired supervision,” *IEEE transactions on image processing*, vol. 30, pp. 2340–2349, 2021.

[28] Z. Cui, K. Li, L. Gu, S. Su, P. Gao, Z. Jiang, Y. Qiao, and T. Harada, “Illumination adaptive transformer,” *arXiv preprint arXiv:2205.14871*, 2022.

[29] Z. Wang, X. Cun, J. Bao, W. Zhou, J. Liu, and H. Li, “Uformer: A general u-shaped transformer for image restoration,” in *Proceedings of the IEEE/CVF conference on computer vision and pattern recognition*, 2022, pp. 17 683–17 693.

[30] S. W. Zamir, A. Arora, S. Khan, M. Hayat, F. S. Khan, and M.-H. Yang, “Restormer: Efficient transformer for high-resolution image restoration,” in *Proceedings of the IEEE/CVF conference on computer vision and pattern recognition*, 2022, pp. 5728–5739.

[31] H. Jie, X. Zuo, J. Gao, W. Liu, J. Hu, and S. Cheng, “Llformer: An efficient and real-time lidar lane detection method based on transformer,” in *Proceedings of the 2023 5th International Conference on Pattern Recognition and Intelligent Systems*, 2023, pp. 18–23.

[32] Z. Fu, Y. Yang, X. Tu, Y. Huang, X. Ding, and K.-K. Ma, “Learning a simple low-light image enhancer from paired low-light instances,” in *Proceedings of the IEEE/CVF Conference on Computer Vision and Pattern Recognition*, 2023, pp. 22 252–22 261.